Supporting Information

Fluorescence Turn-On Response Amplified by Space Confinement in Metal-Organic Frameworks

*Xue-Mei Yin, Lu-Lu Gao, Peng Li, Ran Bu, Weng-Jie Sun and En-Qing Gao**

Shanghai Key Laboratory of Green Chemistry and Chemical Processes, School of Chemistry and Molecular Engineering, East China Normal University, Shanghai 200062 (P. R. China).

*corresponding author. Email: eqgao@chem.ecnu.edu.cn

Physical Measurements

^{1}H NMR spectra were recorded on a Bruker Advance 400 MHz spectrometer. The FT-IR spectra were recorded in the range 500-4000 cm^{-1} using KBr pellets on a Nicolet NEXUS 670 spectrophotometer. Powder X-ray diffraction (PXRD) at ambient pressure was recorded on a Rigaku D/Max-2500 diffractometer at 35kV, 25mA for a Cu-target tube and a graphite monochromator. UV-vis diffuse reflectance spectra were measured using a SHIMADZU UV-2700 spectrophotometer, with $BaSO_4$ plates as references (100% reflection). Liquid phase fluorescence spectra were recorded on a Hitachi F-4500 spectrofluorometer. Solid fluorescence spectra were obtained using a SHIMADZU RF-6000 spectrofluorometer. Scanning electron microscopy (SEM) was performed on a Hitachi S-4800 microscope. Nitrogen adsorption and desorption isotherm measurements were performed on a Micromeritics ASAP2020 analyzer at 77K. Thermal gravimetric analysis (TGA) was performed on a STA 449 F3 Simultaneous Thermal Analyzer in flowing air at 10°C/min.

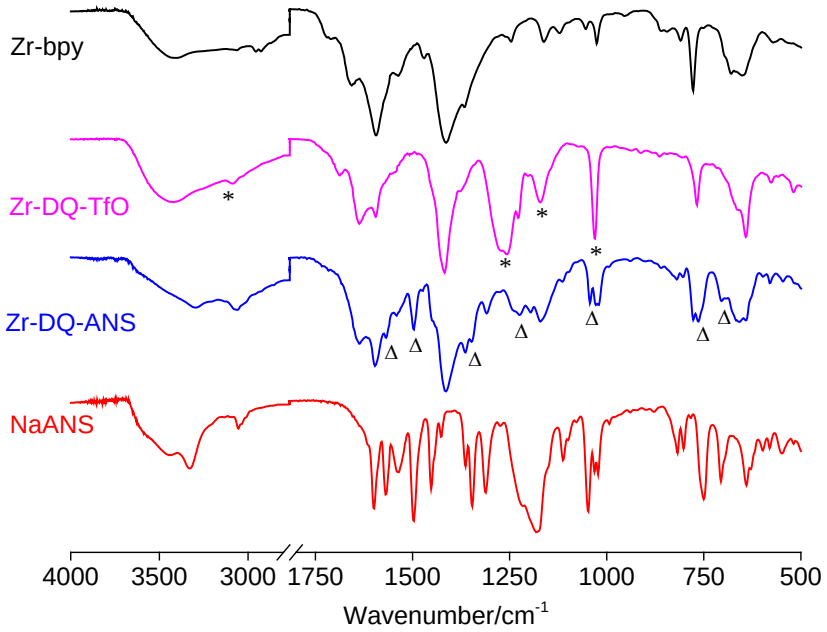

Figure S1. IR spectra of NaANS,, Zr-bpy, Zr-DQ-TfO, and Zr-DQ-ANS. The bands marked with * are new bands of Zr-DQ-TfO compared with Zr-bpy, and those marked with Δ are the bands arising from the ANS^- anion, assigned in comparison with the spectrum of NaANS.

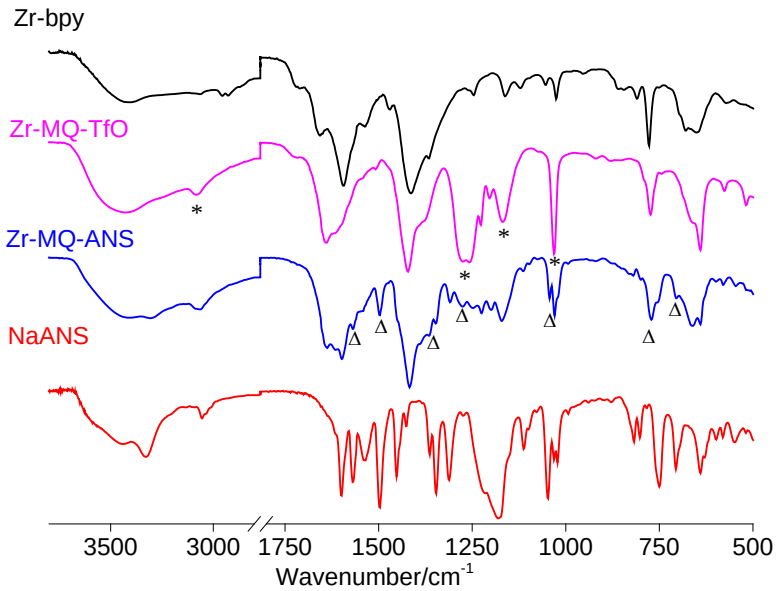

Figure S2. IR spectra of NaANS, Zr-bpy, Zr-MQ-TfO, and Zr-MQ-ANS. The bands marked with * are new bands of Zr-MQ-TfO compared with Zr-bpy, and those marked with Δ are the bands arising from the ANS^- anion, assigned in comparison with the spectrum of NaANS.

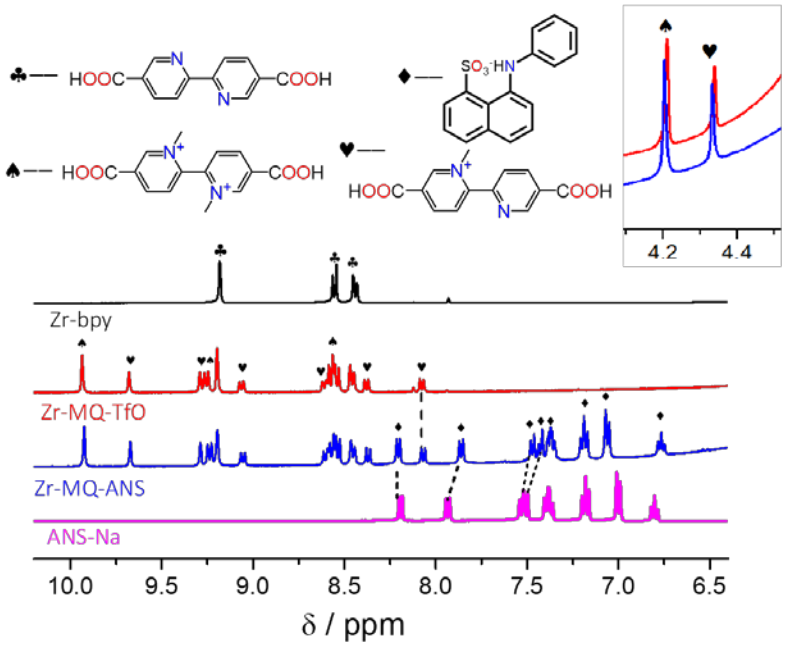

Figure S3. ^{1}H NMR spectra of Zr-DQ-TfO (magenta, N-alkylation ratio: 43%) and Zr-DQ-ANS (blue). The spectra were recorded with the solutions obtained by digesting the solids with HF (aq.)/d_6-DMSO (1/40, v/v).

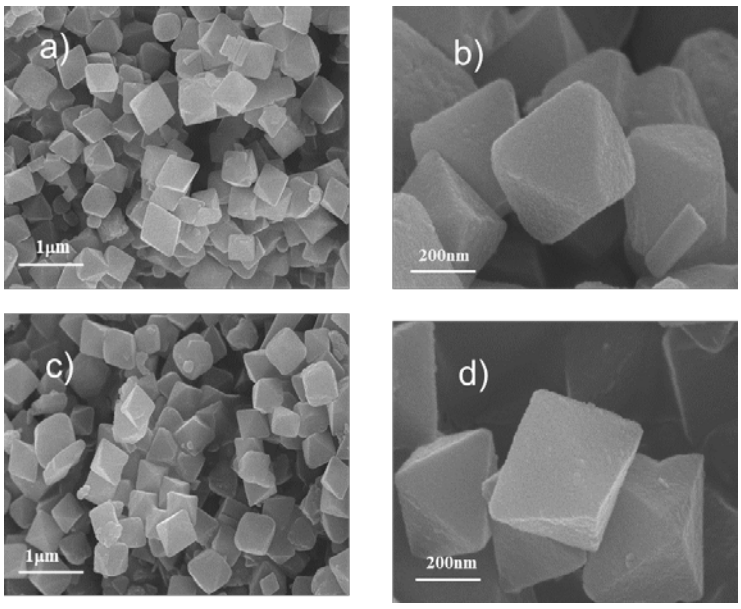

Figure S4. SEM images of Zr-MQ-TfO (a, b) and Zr-MQ-ANS (c, d).

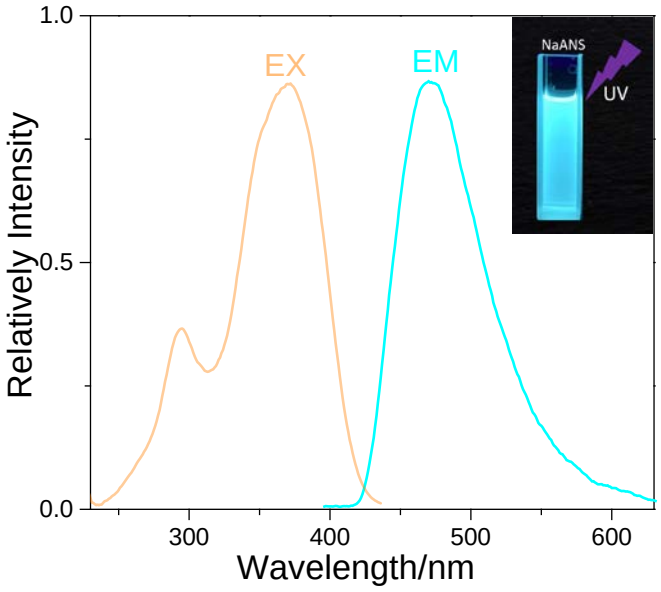

Figure S5. The excitation and emission spectra of NaANS in 1,4-dioxane (0.1 μM).

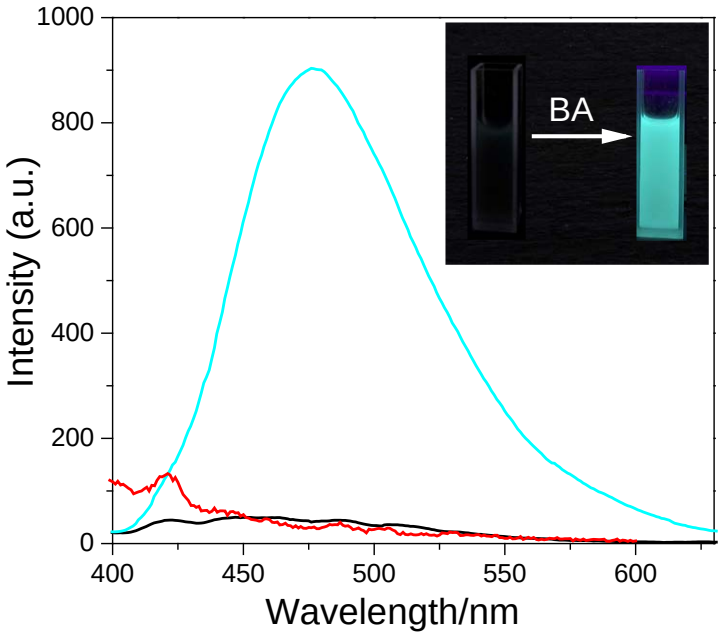

Figure S6. Emission spectra of Zr-MQ-TfO (red), Zr-MQ-ANS (black) dispersions in 1,4-dioxane and that of the Zr-MQ-ANS dispersion after addition of butylamine (BA, 10 μM) (cyan). The inset displays the BA-induced fluorescence turn-on of the Zr-MQ-ANS suspension under UV light (365 nm).

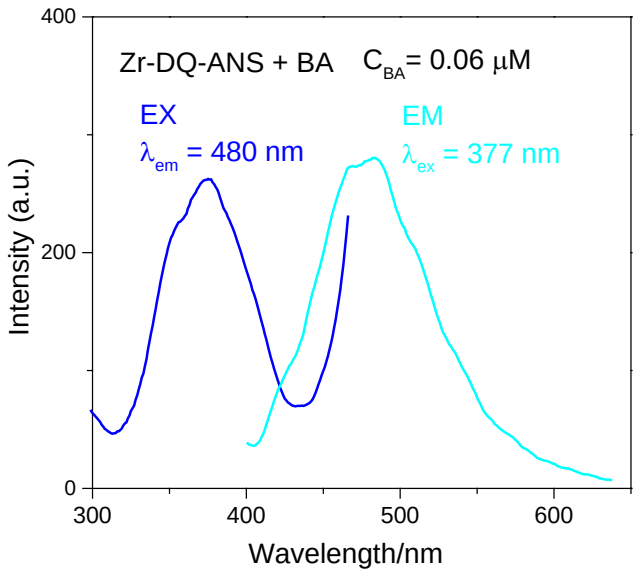

Figure S7. The excitation (blue) and emission spectra (cyan) of Zr-DQ-ANS. (C_{BA}=0.06uM).

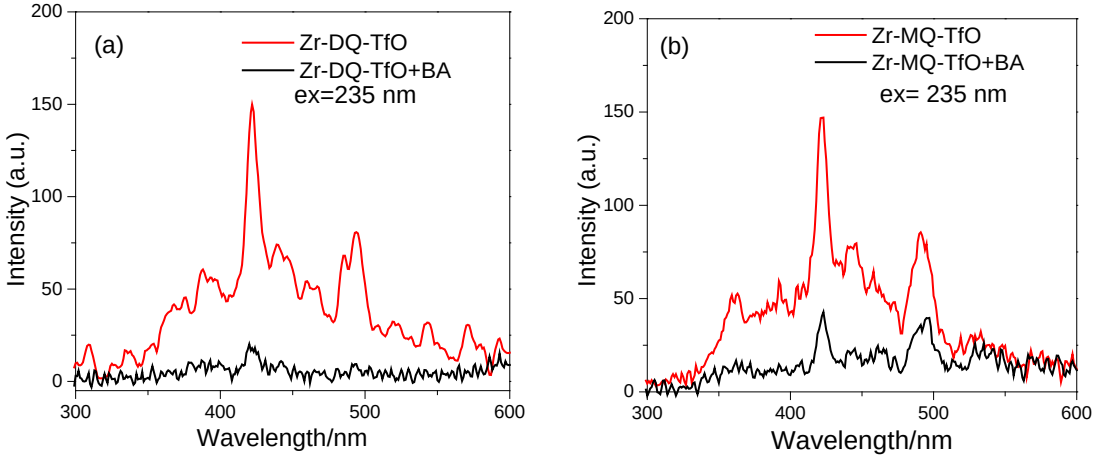

Figure S8. The emission spectra of Zr-DQ-TfO (a) and Zr-MQ-TfO (b) suspensions before and after addition of BA (0.1 M).

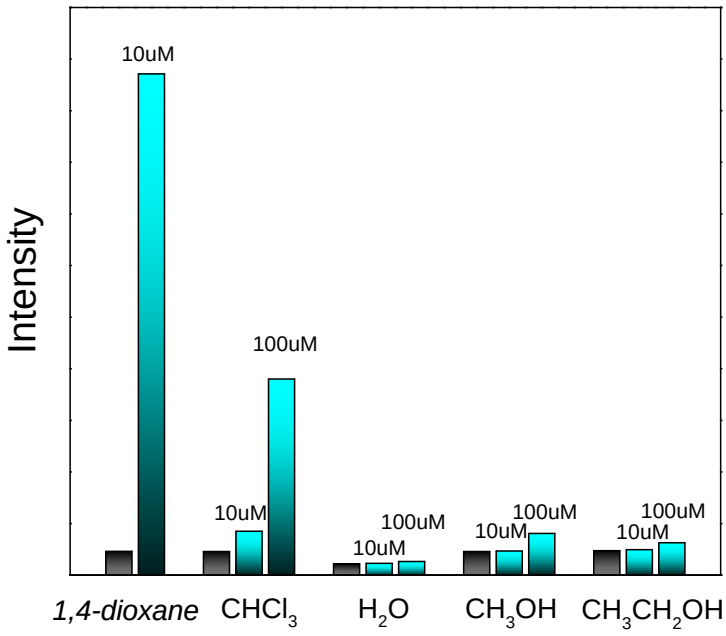

Figure S9. Luminescence intensities of Zr-DQ-ANS suspensions in different solvents in the absence (grey) and presence (cyan) of BA at the specified concentrations.

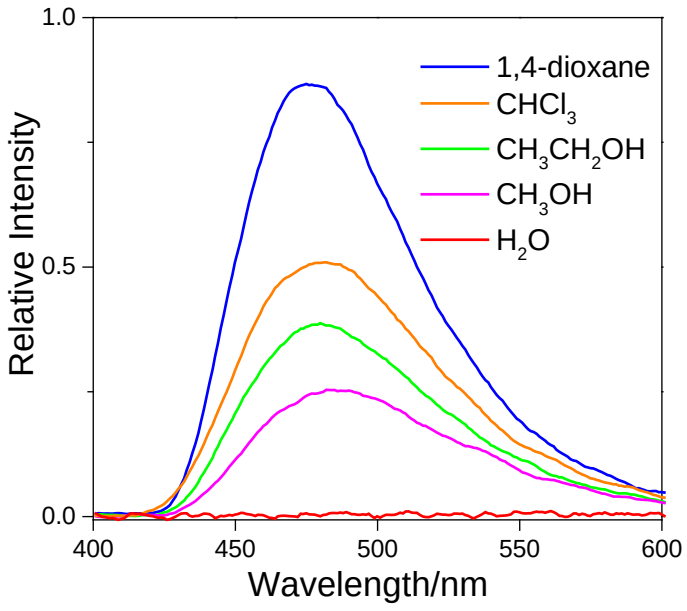

Figure S10. The emission spectra of NaANS in different solvents (λ_{ex}=377 nm).

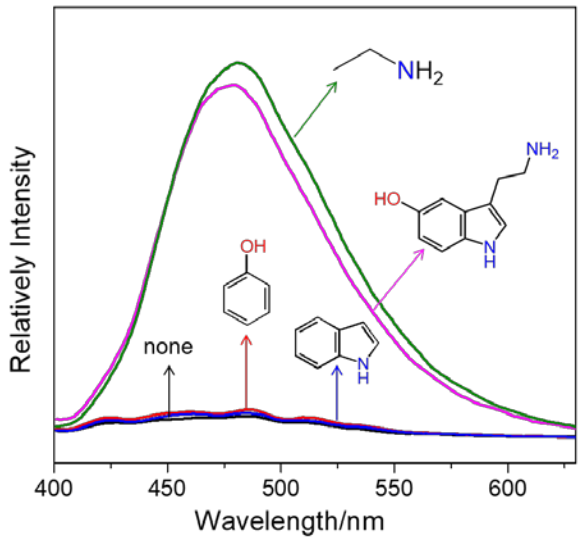

Figure S11. Emission spectra of the Zr-DQ-ANS dispersions in response to phenol, indole ethylamine and 5-HT (10 μM).

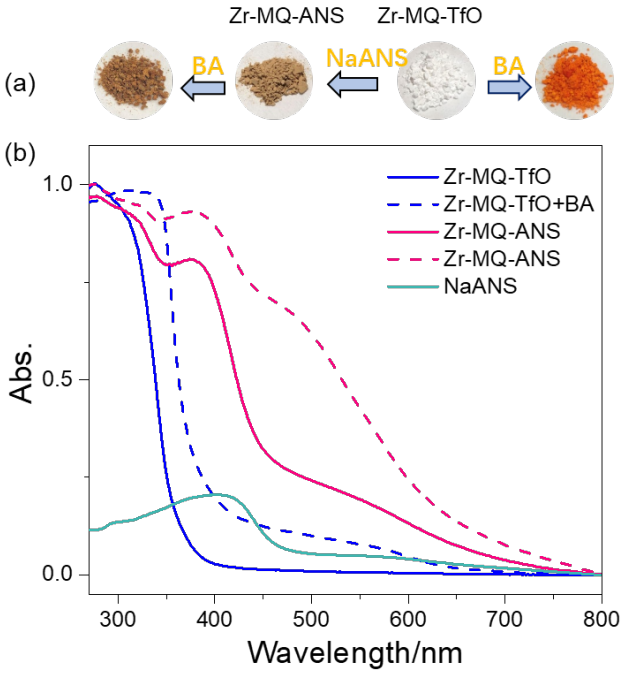

Figure S12. (a) Photographs showing the color changes before and after treating Zr-DQ-TfO and Zr-DQ-ANS with pure BA. (b) Normalized solid-state UV-vis spectra of Zr-DQ-TfO and Zr-DQ-ANS before (solid lines) and after (dashed lines) BA treatment. For comparison, the spectrum of NaANS is included.

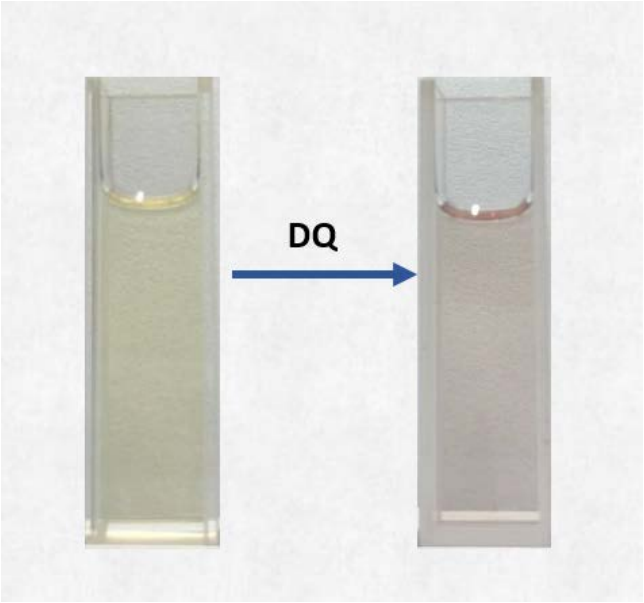

Figure S13. Photograph of color change before and after addition of $[Me_2DQdc]^{2+}$to NaANS 1,4-dioxane solution.

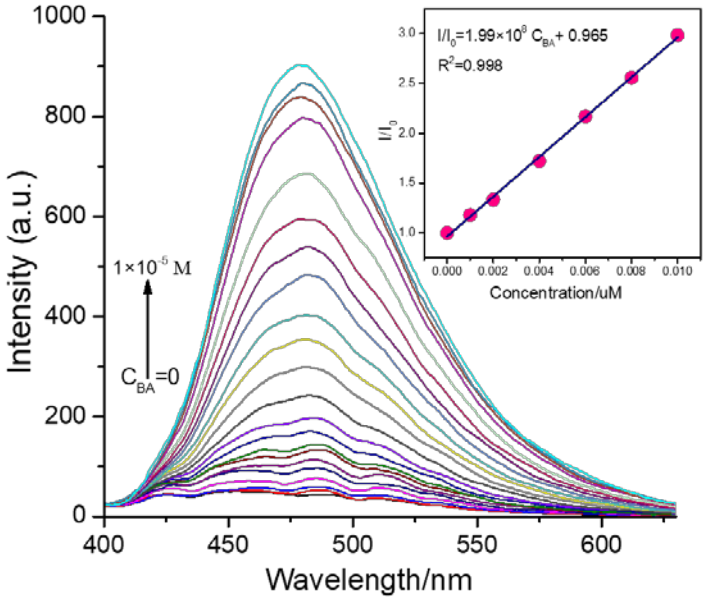

Figure S14. Emission spectra of the Zr-MQ-ANS dispersion in presence of different BA concentrations (λ_{ex}=377 nm). Inset: linear variation of I/I_0 (at 480 nm) with BA concentration in the low concentration region.

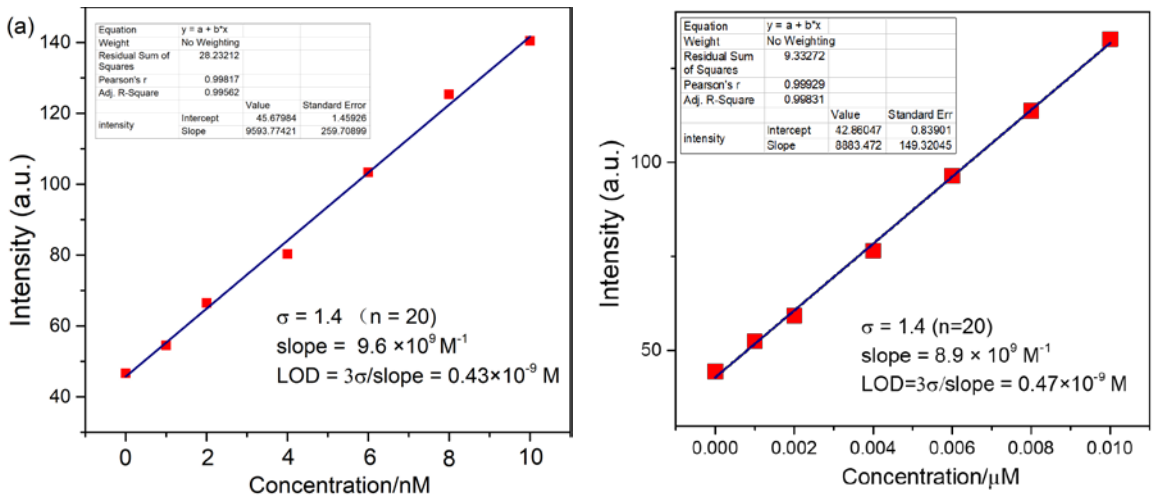

Figure S15. Data for calculations of LODs. The linear fit of the intensity-concentration data in low butylamine concentration range is shown. Left: Zr-DQ-ANS. Right: Zr-MQ-ANS.

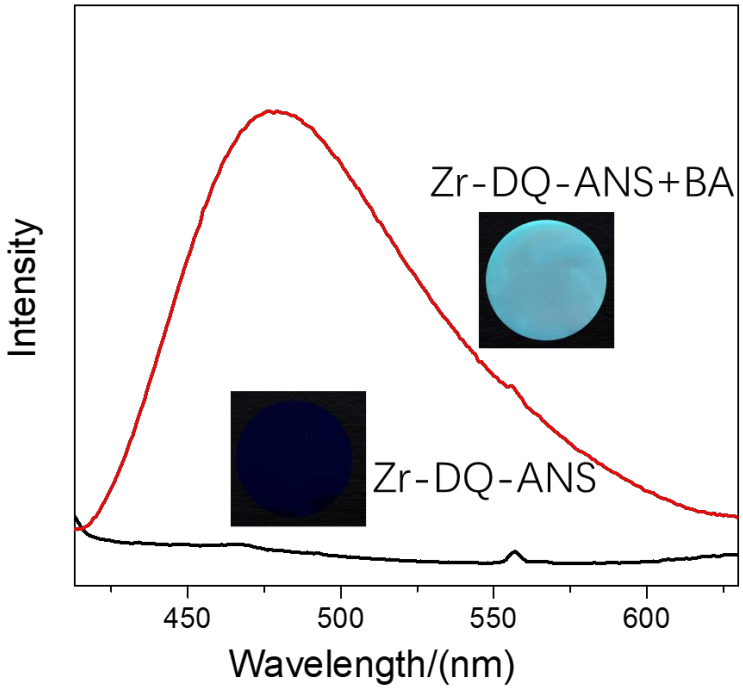

Figure S16. Solid-state emission spectra of Zr-DQ-ANS before (black) and after (blue) exposure to butylamine (BA) (λ_{ex} = 377 nm).

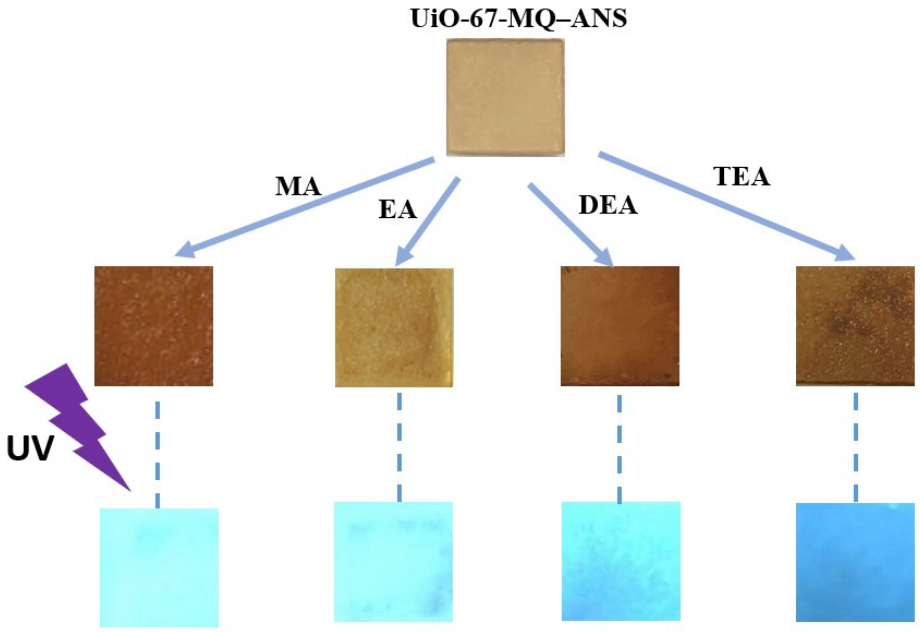

Figure S17. Photographs of the quartz slide supported Zr-MQ-ANS layers before and after treated with different amines: top and middle, under natural lights; bottom, under UV light (365nm). MA = methylamine, EA = ethylamine, DEA = diethylamine, TEA = triethylamine.

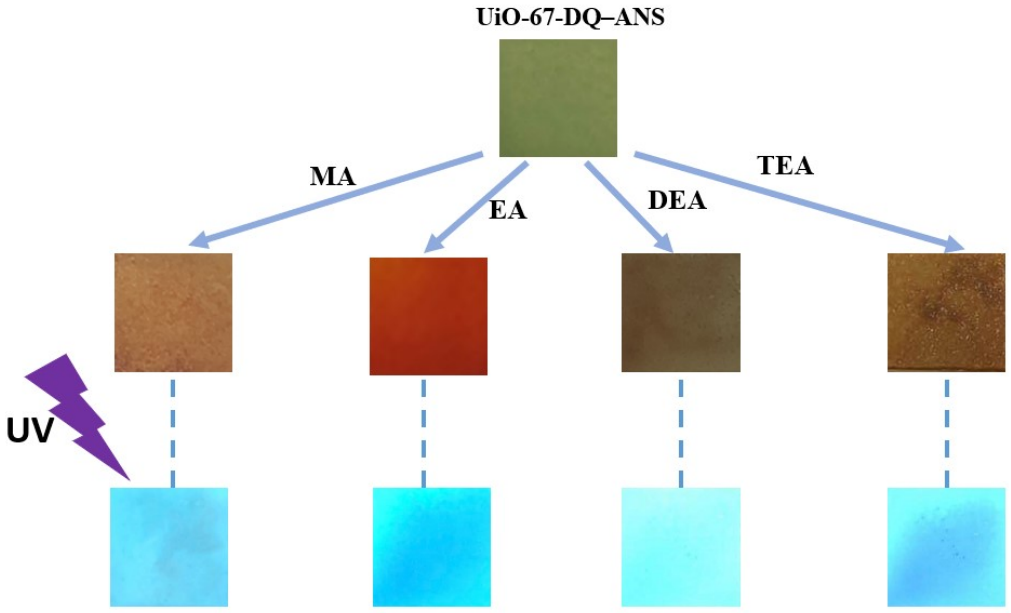

Figure S18. Photographs of Zr-DQ-ANS encounters different amines resulting in color changes and fluorescence under UV light (365nm). MA = methylamine, EA = ethylamine, DEA = diethylamine, TEA = triethylamine.